THE JOURNAL OF BIOLOGICAL CHEMISTRY
Vol. 277, No. 33, Issue of August 16, pp. 29608–29616, 2002

*Printed in U.S.A.*

# Characterization of a Hyperthermophilic P-type ATPase from *Methanococcus jannaschii* Expressed in Yeast*

Received for publication, April 22, 2002, and in revised form, May 31, 2002
Published, JBC Papers in Press, June 4, 2002, DOI 10.1074/jbc.M203871200

**Pierre Morsomme‡§¶, Mohamed Chami§‖, Sergio Marco‖, Joseph Nader‡, Karen A. Ketchum**‡‡, André Goffeau‡§§, and Jean-Louis Rigaud‖**

*From the ‡Unité de Biochimie Physiologique, Université Catholique de Louvain, Place Croix du Sud 2-20, B-1348 Louvain-la-Neuve, Belgium, ‖Institut Curie, UMR-CNRS 168 and LRC-CEA, 11 Rue Pierre et Marie Curie, 75231 Paris, France, **Institute for Genomic Research, Rockville, Maryland 20850*

**We report on the biochemical and structural properties of a putative P-type $H^+$-ATPase, MJ1226p, from the anaerobic hyperthermophilic Archaea *Methanococcus jannaschii*. An efficient heterologous expression system was developed in *Saccharomyces cerevisiae* and a four-step purification protocol, using *n*-dodecyl β-D-maltoside, led to a homogenous detergent-solubilized protein fraction with a yield of over 2 mg of protein per liter of culture. The three-dimensional structure of the purified detergent-solubilized protein obtained at 2.4 nm resolution by electron microscopy showed a dimeric organization in which the size and the shape of each monomer was compatible with the reported structures of P-type ATPases. The purified MJ1226p ATPase was inactive at 40 °C and was active at elevated temperature reaching high specific activity, up to 180 μmol of $P_i \cdot min^{-1} \cdot mg^{-1}$ at 95 °C. Maximum ATPase activity was observed at pH 4.2 and required up to 200 mM monovalent salts. The ATPase activity was stable for several days upon storage at 65 °C and was highly resistant to urea and guanidine hydrochloride. The protein formed catalytic phosphoenzyme intermediates from MgATP or $P_i$, a functional characteristic specific of P-type ATPases. The highly purified, homogeneous, stable, and active MJ1226p ATPase provides a new model for further structure-function studies of P-type ATPases.**

The ability of Archaea to grow in extreme habitats has led to the exploration of the molecular mechanisms that confer stability to proteins under high temperature, high pressure, or extreme pH values. The basis of thermotolerance of the bioenergetic features of archaeal species is particularly intriguing. As in bacterial cells, membrane-residing systems in anaerobic Archaea use an electrochemical potential of either hydrogen ions or sodium ions for primary energy conservation (1). However, in archaeal methanogens, simultaneous primary gradients of both protons and sodium ions can be used to drive ATP synthesis (2). Until recently, P-type ATPases were not suspected to be responsible for the generation of the primary electrochemical potential across archaeal membrane. This possibility has to be revisited because of the discovery through genome sequencing of several P-type ATPase genes. From the seven archaeal genome sequences annotated so far, 18 genes encoding P-type ATPases have been identified (axe@biobase.dk and www-biology.ucsd.edu/~ipaulsen/transport/). Most archaeal P-type ATPases belong to the bacterial families of potassium- or metal-transporting P-type ATPases. However, four archaeal P-type ATPase sequences cluster with eucaryotic phylogenetic families. Among them, two new members of the family of $H^+$-ATPases were identified in *Methanococcus jannaschii* (3) and *Thermoplasma acidophilum* genome (4), respectively. This observation is intriguing because $H^+$-transporting P-type ATPases were believed to be restricted to yeast (5, 6), fungi (7, 8), and plants (9, 10).

Unfortunately, very few archaeal P-type ATPases have been characterized biochemically, and only one of them, the thermophilic $Ag^+/Cu^+$ ATPase from *Archaeoglobus fulgidus*, has been purified after expression in *Escherichia coli* (11). One of the main limiting factors is the inability to produce large amounts of pure transport protein from archaeal genes. Although heterologous expression systems have proven to be useful for phenotypic characterization of proteins that often cannot be produced in their original host, heterologously expressed membrane proteins are often of limited activity, and their purification in large scale is still cumbersome. Therefore, development and/or improvement of cloning systems for the heterologous production of large amounts of pure and stable transport proteins from archaeal genes would be of considerable interest.

In this study, we describe the cloning, heterologous expression, purification, and biochemical and structural characterization of MJ1226p, a putative P-type $H^+$-ATPase of the anaerobic hyperthermophilic Archaea *Methanococcus jannaschii*. MJ1226p was expressed in the yeast *Saccharomyces cerevisiae* using a cloning system that was shown to be suitable for heterologous expression of mammal, plant, and fungi P-type ATPases (12–19). A purification process, based on the hyperthermostability of the enzyme and the presence of a six-histidine tag, allowed large scale production of a highly purified protein. The purified MJ1226p ATPase activity was found to be thermophilic up to 95 °C. Its full activity required monovalent salts and acidic pH. The ATPase activity was highly resistant to denaturation by temperature or chaotropic agents such as urea and guanidine hydrochloride. It was able to form catalytic phosphoenzyme intermediates from both MgATP and $P_i$, a functional characteristic specific of P-type ATPases. The three-dimensional structure, of the purified detergent-solubilized

* This work was supported by grants from the Interuniversity Pôle d'Attractions program of the Belgian Government Office for Scientific, Technical, and Cultural Affairs (to A. G.), Fonds National de la Recherche Scientifique (to P. M.), and the Chaire Internationale de Recherche Blaise Pascal (to M. C.). The costs of publication of this article were defrayed in part by the payment of page charges. This article must therefore be hereby marked "*advertisement*" in accordance with 18 U.S.C. Section 1734 solely to indicate this fact.

§ Both authors contributed equally to this work.
¶ Present address: Biozentrum, University of Basel, Klingelbergstrasse 70, CH-4056 Basel, Switzerland.
‡‡ Present address: Celera, 45 West Gude Dr., Rockville, MD 20850.
§§ To whom correspondence should be addressed. Tel.: 3210473614; Fax: 3210473872; E-mail: goffeau@fysa.ucl.ac.be.

protein, obtained at 2.4 nm resolution by electron microscopy showed a dimeric organization, in which each monomer compared well with the reported structures of the SERCA calcium ATPase, a prototypical P-type ATPase (20, 21). This study demonstrates that the MJ1226p ATPase of the hyperthermophilic *M. jannaschii* provides new possibilities for the functional and structural analysis of P-type ATPases. It also provides new insights into the thermostability of ion transport proteins, the bioenergetics of archaea, and the phylogeny of P-type plasma membrane $H^+$-ATPases.

## MATERIALS AND METHODS

*Plasmid Constructions*—The *MJ1226* open reading frame containing 2,415 nucleotides, and coding for a putative plasma membrane $H^+$-ATPase was obtained from two overlapping clones AMJFO85 (contained the 5′ end to nucleotide 2291) and AMJGG15 (started from position 167 and extended to the 3′ end) (3). The 5′ end of the gene was amplified from the AMJFO85 clone by PCR using the following oligonucleotides: MJ1 (GGAATTCATGTGGGGGGTTGTTATGATTGT) and MJ3 (CTCCAATCCTAATTCTAACAA). The PCR product was then inserted in the *Eco*RI/*Eco*RV site of the AMJGG15 clone in order to reconstitute the full-length *MJ1226* open reading frame. A $His_6$-tagged version of the *MJ1226* open reading frame was obtained with the same strategy using the MJ2 oligonucleotide (GGAATTCATGCATCACCATCACCATCACTGGGGGGTTGTTATGAATGTTGAG) instead of MJ1. The $His_6$ tag was thus inserted at the amino-terminal end, between the 1st and 2nd residue of the protein. All the constructions were verified by sequencing. The coding sequence of *MJ1226* was inserted between the yeast *PMA1* promoter and the *ADC1* terminator in a 2-$\mu$m multicopy vector, derived from Yeplac181 (22) by a strategy similar to that described by de Kerchove d'Exaerde *et al.* (15). The multicopy expression plasmids with the *PMA1* promoter and *ADC1* terminator were named MJ1p and MJ2p for the untagged and tagged version of MJ1226, respectively.

*Yeast Strains*—The YAK2 strain (*Mat**a**, ade2-101, leu2-Δ1, his3-Δ200, ura3-52, trp1Δ63, lys2-801, pma1-Δ::HIS3, pma2-Δ::TRP1*) has the chromosomal $H^+$-ATPase genes, *PMA1* and *PMA2*, deleted and the essential *PMA1* gene under the control of the inducible *GAL1-10* promoter on an *URA3* centromeric plasmid (15). Yeast cells were transformed according to Ito *et al.* (23).

*Crude Membrane Preparation*—YAK2 cells transformed with either the MJ1226-containing plasmid (MJ1p or MJ2p) or the Yeplac181 (empty) plasmid were grown on a 2% (w/v) galactose medium depleted of His, Leu, Ura, and Trp. Cells were grown in liquid medium until they reached a density of $20.10^6$ cells/ml. *MJ1226* expression was induced by growing the cells in medium with 2% (w/v) glucose for 16 h. Cells were then harvested, washed twice with ice-cold water, and resuspended in 250 mM sorbitol, 1 mM $MgCl_2$, 50 mM imidazole NaOH, pH 7.5, 1 mM phenylmethylsulfonyl fluoride, 5 mM dithiothreitol, and the protease inhibitors leupeptin, aprotinin, antipain, pepstatin, and chymostatin at 2 $\mu$g/ml each. Cells were broken in the presence of glass beads as described in Goffeau and Dufour (24). Two centrifugations, the first at 3,500 rpm (SS34) for 5 min and the second at 6,000 rpm for 5 min, were followed by a third centrifugation at 21,500 × *g* for 40 min to obtain a crude particulate fraction. The pellet was resuspended in a buffer containing 10 mM imidazole, pH 7.5, 1 mM $MgCl_2$, and protease inhibitors. Fractions were aliquoted, frozen in liquid nitrogen, and stored at −80 °C. The protein concentration was determined by the method of Lowry *et al.* (25).

*Solubilization and Purification of MJ1226p*—Twenty five mg of crude particulate fraction in 4 ml was solubilized with *n*-dodecyl β-D-maltoside (DDM)[1] at a detergent-to-protein ratio of 2:1 (w/w). The sample was thoroughly mixed at room temperature for 10 min and then centrifuged for 1 h at 100,000 × *g*. The supernatant was incubated for 5 min at 95 °C, cooled in ice, and centrifuged again for 1 h at 100,000 × *g*. The new supernatant was incubated at room temperature with 1 ml of $Ni^{2+}$-nitrilotriacetic (Ni-NTA) resin (Qiagen) for 3 h on a rotary wheel. The matrix was loaded into a column, washed 5 times with 1 ml of buffer containing 20 mM imidazole, pH 7.5, 1 mM $MgCl_2$, 150 mM KCl, 10% (w/v) glycerol, 0.05% (w/v) DDM. Proteins were eluted with 250 mM imidazole, pH 7.5, 1 mM $MgCl_2$, 150 mM KCl, 10% glycerol, 0.05% DDM.

*Size-exclusion Chromatography*—Ni-NTA purified fractions of MJ1226p were concentrated on Amicon ultrafiltration membrane (cut-off 50 kDa) up to 2–3 mg of protein/ml. An aliquot of 100 $\mu$l was loaded on a Superose 6 (Amersham Biosciences) column, equilibrated, and eluted with 20 mM Mes-KOH, pH 6.5, 100 mM NaCl, 1 mM $MgCl_2$, 0.05% DDM, 10% glycerol. Fractions of 500 $\mu$l were harvested and analyzed for protein content.

*ATPase Assays*—Standard ATPase assays were performed in the presence of 6 mM MgATP, 50 mM Mes-KOH, pH 5.0, 200 mM potassium acetate, 0.1% DDM, and 0.3 $\mu$g of protein at 95 °C for 3 min. The pH of this reaction medium at 95 °C was 4.2. The reaction was started by quickly raising the temperature from room temperature to 95 °C and was stopped by addition of 1% SDS. The activity of MJ1226p was defined as the difference between the activity measured in the MJ1226p fraction and the activity measured either in a similar fraction obtained from the control strain expressing the empty plasmid or with the MJ1226p fraction treated with 1% SDS before incubation at 95 °C.

*Phosphoenzyme Formation*—Formation of phosphoenzyme intermediates by ATP was carried out at 0, 30, or 65 °C by incubating 10 $\mu$g of purified *MJ1226p* in 0.2 ml of 20 mM citric acid, pH 5.0, 80 mM KCl, 5 mM $MgCl_2$, 0.05% asolectin. The phosphorylation reaction was started by addition of 2 mM [$\gamma$-$^{32}$P]ATP and stopped 10 s later by the addition of 50 ml of 50% (w/w) ice-cold trichloroacetic acid, 100 mM ATP, 100 mM $MgCl_2$. Inhibition of phosphorylation was checked by adding 10 mM ATP or 10 mM hydroxylamine 10 s after the reaction was started, and a further 10-s incubation was performed before trichloroacetic acid addition. Precipitated proteins were collected by centrifugation, washed three times with 20 mM $KH_2PO_4/H_3PO_4$, pH 2.0, 20 mM ATP, 10% trichloroacetic acid, and analyzed by cationic detergent/polyacrylamide gel electrophoresis at acid pH as described (26). After electrophoresis, gels were dried and subjected to autoradiography. The gels were then rehydrated and stained with Coomassie Blue to visualize the amount of protein loaded on the gel.

Phosphoenzyme formation by inorganic phosphate ($P_i$) was carried out at 65 °C by first incubating 10 $\mu$g of purified MJ1226p in 0.2 ml of 20 mM citric acid, pH 5.0, 5 mM $MgCl_2$, 0.05% asolectin. When indicated, 10 mM vanadate was added. The phosphorylation reaction was started by addition of 5 mM $^{32}P_i$ and stopped 10 min later by the addition of 50 ml of 50% ice-cold trichloroacetic acid, 10 mM $KH_2PO_4$. Precipitated proteins were collected by centrifugation, washed three times with 1 mM $KH_2PO_4$, 10% trichloroacetic acid, and analyzed as described previously.

*Single Particle Analysis and Three-dimensional Reconstruction*—Purified protein was diluted to about 0.05 mg of protein/ml in a buffer containing 10 mM Tris, pH 7.4, 50 mM NaCl, and 0.05% DDM. Aliquots were deposited onto 400 mesh glow discharged carbon-coated grids and stained with 1% uranyl acetate. Untilted electron micrographs and 45° tilted pairs of MJ1226p were recorded at an accelerating voltage of 120 kV and a magnification of 45,000, using a low dose system, in a Philips CM120 electron microscope. All micrographs were recorded on Kodak SO-163 films. The focus values were −1.6 $\mu$m for tilted pairs and −0.8 $\mu$m for untilted images. Micrographs were digitized at 0.5 nm/pixel using a Leafscan 45 digitizer. A total number of 546 image pairs were windowed and centered by using X-MIPP software (27) and PSPC algorithm (28) before classification. Self-organizing Kohonen neural network (29) and multivariate statistical analysis (30, 31) were performed over untilted images to identify homogeneous groups of projections. Average image of the major group was computed to perform a first three-dimensional reconstruction using SPIDER software (32). This volume was used as reference for angular assignment and refinement of 1464 cryo-microscopic untilted images, which were used to compute the final three-dimensional reconstruction of frozen-hydrated protein (33). Samples for cryo-microscopy were prepared on liquid ethane at −178 °C using a CPC station (Leica). Frozen grids were transferred into a Philips CM120 electron microscope using a Gatan 626 cryo-station before image recording under the same conditions as those described above for negatively stained samples. Final volume was filtered at the resolution estimated by FRC method (34). Volume rendering was performed using ETDIPS version 2 software (35).

After three-dimensional reconstruction computation, x-ray structure of the $Ca^{2+}$-ATPase was docked into the volume obtained by electron microscopy by filtering the atomic structure at 2.4 nm resolution and searching for the best matching positions into the volume of a MJ1226p monomer using SPIDER software (32).

[1] The abbreviations used are: DDM, *n*-dodecyl β-D-maltoside; CHAPS, 3-[(3-cholamidopropyl)dimethylammonio]-1-propanesulfonic acid; Ni-NTA, $Ni^{2+}$-nitrilotriacetic acid; TM, transmembrane; Mes, 4-morpholineethanesulfonic acid; SERCA, sarcoplasmic reticulum calcium-ATPase.

**M4**

```
MJ1226          258   FALVLAVSAIPAAMPAVLSIT   296
AHA2            274 IDNLLVLLIGGIPIAMPTVLSVT   278
BINDING Hydr          --------IG-I----------
CONSENSUS H+          ----L---I-G-P---P-V---T

CONSENSUS Ca++        F---V-LAVAAIPEGLPAV-T--
BINDING Ca++          ------LA---I-E---------
```

**M5**

```
MJ1226          615  SYVIYRITETIRILFFVELCILI  636
AHA2            644  NYTIYAVSITIRIVFGFMLIALI  666
BINDING Hydr          ------------------------
CONSENSUS H+          -Y--Y-------------L---I

CONSENSUS Ca++        -FIRY--S-N-GE---I------
BINDING Ca++          ---------N--E----------
```

**M6**

```
MJ1226          641 ITALMIVLLAILNDIPILAIAYD  663
AHA2            671 FSAFMVLIIAILNDGTIMTISKD  693
BINDING Hydr          -------------D---------
CONSENSUS H+          --------IAI--D-----I-D

CONSENSUS Ca++        L-P-Q-LW-NLVTDG-PA-ALG-
BINDING Ca++         ----------N--TD---------
```

FIG. 1. **Amino acid sequence alignment of predicted transmembrane helices of P-type ATPases.** Spans 4–6 are from MJ1226p, SERCA $Ca^{2+}$-ATPase, and plant plasma membrane $H^+$-ATPase AHA2. The consensus sequences for proton and calcium P-type ATPases are from Palmgren (51). The nine residues from TM 4–6 shown to be involved in the binding of calcium ions in SERCA are from Toyoshima *et al.* (21). The four residues proposed to bind the hydronium (*Hydr.*) ion to AHA2 are from Bukrinsky *et al.* (37).

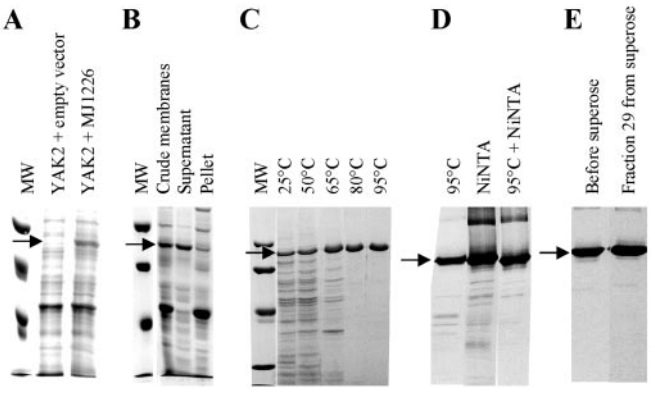


FIG. 2. **Expression and purification of MJ1226p examined on SDS-PAGE.** *A*, crude membrane fraction of uninduced (*2nd lane*) and induced (*3rd lane*) *S. cerevisiae*. *B*, selective solubilization by DDM of MJ1226p from induced yeast membranes. *C*, selective enrichment in MJ1226p following heat treatment of the DDM solubilized fraction for 5 min. *D*, comparison of MJ1226p purification by heat treatment (*1st lane*), Ni-NTA chromatography (*2nd lane*), and heat treatment followed by Ni-NTA chromatography (3*rd lane*). *E*, size-exclusion chromatography on Superose 6 of MJ1226p after heat treatment and Ni-NTA chromatography. The 84-kDa protein is indicated by an *arrow*. *MW,* molecular weight markers. *A–C* are Coomassie Blue-stained gels. *D* and *E* are silver-stained gels.

## RESULTS

*Sequence Analysis*—Genome analysis of the hyperthermophile *M. jannaschii* revealed the presence of a putative P-type $H^+$-ATPase, named MJ1226p. Blast analysis of this sequence showed high sequence similarity with plant and yeast plasma membrane $H^+$-ATPases. The 80 closest orthologues of MJ1226p, ranging from similarity *E* scores of $e^{-157}$ to $e^{-86}$, were established plant, fungal, and ciliate plasma membrane $H^+$-ATPases. The closest non-$H^+$-ATPase was a putative $Ca^{2+}$-ATPase from *Clostridium perfringens* with a much lower similarity (*E* score of $e^{-85}$).

Alignment analysis showed that MJ1226p (805 residues) shared 41 and 39% identity with the *Nicotiana plumbaginifolia* PMA4 (952 residues) and the *Schizosaccharomyces pombe PMA1* (919 residues) plasma membrane $H^+$-ATPases, respectively. The MJ1226p P-type ATPase has therefore been phylogenetically classified among the family of plasma membrane $H^+$-ATPases (36). The recently identified TA1045p (787 residues) from the Archaea *T. acidophilum,* which has 39% identity to the *MJ1226* gene product from *M. jannaschii,* makes with the latter a distinct two-member phylogenetic cluster in the proton-ATPase family. The amino- and carboxyl-terminal ends of MJ1226p are shorter compared with plant and yeast $H^+$-ATPases, but no significant differences can be detected throughout the rest of the sequence.

Fig. 1 shows the alignments of the predicted transmembrane domains 4–6, which compose the $Ca^{2+}$-binding sites of the SERCA P-type ATPase (21). Among the 70 residues of TM 4–6 from MJ1226p, a total of 14 residues were strictly conserved in most plants and fungal proton ATPases. On the other hand, 11 residues were conserved in an alignment with the TM 4–6 from the SERCA $Ca^{2+}$-ATPases, but only 3 among the 9 residues ligating the $Ca^{2+}$ ions in SERCA were conserved in MJ1226p. It has been speculated recently (37) that the hydronium-binding site of the plant AHA2p ATPase composes Asp-684 in TM 6 (which is conserved as D654 in MJ1226p) and the three carbonyls from Ile-282, Gly-283, and Ile-285 in TM 4 (which become Val-264, Ser-265, and Ile-267, in MJ1226p). In this hypothesis, only two of the four postulated hydronium-binding residues of AHA2p would be conserved in MJ1226p. All together, these phylogenetic analyses render it unlikely that MJ1226p is a $Ca^{2+}$-ATPase but do not prove that MJ1226p is a proton-ATPase.

*Expression of the Archaebacterial MJ1226 Protein in Yeast*—We have expressed the archaeal *MJ1226* gene in the yeast *S. cerevisiae* using a cloning system, which was shown to be suitable for heterologous expression of plant and fungi plasma membrane $H^+$-ATPases (15, 16, 38). We used a yeast strain deleted of its own plasma membrane $H^+$-ATPase genes, *PMA1* and *PMA2*. This strain was able to survive on galactose medium due to the presence of *PMA1* under the control of the *GAL1–10* promoter on a *URA3* centromeric plasmid (15). This strain was transformed with either a multicopy plasmid carrying the *M. jannaschii MJ1226* gene or with the empty plasmid Yeplac181. The ability of the archaeal *MJ1226* gene to replace the yeast *PMA1* was tested by replicating transformants from galactose to glucose medium containing 5-fluoro-orotic acid to chase the plasmid containing the *PMA1* and *URA3* genes. Under these conditions, transformants replicated on glucose medium were unable to grow at 30 °C indicating that at this temperature the Archaea gene was not able to replace the yeast *PMA1*.

The Archaea *MJ1226* protein was well expressed in yeast membrane fractions as observed on Coomassie Blue-stained SDS-PAGE gel. A major band at 84 kDa appeared in crude particulate fractions of the yeast strain expressing MJ1226p compared with the control strain (Fig. 2*A*). Additional evidence for the good expression of *MJ1226* relies on a comparison of the temperature dependence of the total hydrolytic ATPase activities of crude membranes from yeast cells expressing either the empty vector or the *MJ1226*-containing plasmid. Two peaks of ATPase activity were detected at 50 °C and above 90 °C in the strain expressing MJ1226p, whereas only one peak was detected at 50 °C in the control strain (see below Fig. 4*A*). The peak observed at 50 °C in both strains should correspond to the

TABLE I
*Purification of MJ1226p ATPase from 1.5 liters of yeast culture*

| Steps | Protein | ATPase units | ATPase-specific activity |
|---|---|---|---|
| | *mg* | $\mu mol \cdot min^{-1}$ | $(\mu mol \cdot min^{-1} \cdot mg^{-1})$ |
| Crude membranes | 619 | 3264 | 5 |
| Solubilization | 279 | 2990 | 11 |
| Heat shock | 52 | 2630 | 51 |
| NiNTA | 9 | 1290 | 143 |
| Superose 6 | 2.5 | 438 | 175 |

yeast Pma1p activity. On the contrary, the peak observed above 90 °C corresponds to the overexpressed MJ1226p because it was not detected in the control strain.

*Solubilization and Purification of MJ1226p*—Solubilization of yeast membrane fractions with 1.25% DDM allowed a significant enrichment of the 84-kDa protein as shown in gel electrophoresis (Fig. 2*B*). Heat treatment of the total solubilized extract for 5 min above 80 °C induced precipitation of protein contaminants and considerable purification of the 84-kDa band. As shown in Fig. 2*C*, only faint contaminant proteins could be detected on an SDS gel loaded with 10 $\mu$g of heat-treated proteins. The heat shock treatment was remarkably efficient because over 80% of the ATPase units from the crude particulate fraction were recovered, whereas the specific activity was multiplied by a factor of 10 (Table I). For comparison, purification of the total solubilized extract by Ni-NTA chromatography also allowed exhaustive purification of the 6His-MJ1226p, but several minor contaminants could be detected (Fig. 2*D*). Finally, the combination of the heat treatment followed by a Ni-NTA chromatography led to the production of a highly purified 84-kDa protein. Only a weak high molecular weight component of unknown nature could be detected on silver-stained SDS-PAGE (Fig. 2*D*). Noteworthy, the Ni-NTA chromatography step after the heat treatment led to a 3-fold increase of the specific ATPase activity (Table I). Control experiments indicated that this increase could not be related to the removal of some detergent that could have been heat-denatured. Most probably, the marked increase of ATPase-specific activity by Ni-NTA chromatography was due to the separation in the flow-through fraction of a form of the enzyme with no affinity to Ni-NTA and with a much lower ATPase activity (25 $\mu mol \cdot min^{-1} \cdot mg^{-1}$) (data not shown) than that of the fraction eluted by 250 mM imidazole (150 $\mu mol \cdot min^{-1} \cdot mg^{-1}$).

Homogeneity of the 84-kDa band from the heat plus Ni-NTA fraction was analyzed by size-exclusion chromatography on a Superose 6 column leading to three protein peaks eluting at fractions 26, 29, and 31, respectively. Each of these peaks exhibited only the 84-kDa protein band as determined by silver-stained SDS-PAGE (Fig. 2*E*, *fraction 29*). The specific ATPase activity was moderately enhanced in the fraction 29 (175 $\mu mol \cdot min^{-1} \cdot mg^{-1}$) as compared with those measured in the two other Superose 6 peaks (100 $\mu mol \cdot min^{-1} \cdot mg^{-1}$). The major peak from fractions 28–30 was pooled and found to contain about 10 mol of endogenous phospholipids per mol of protein as determined by the method of Dufour and Goffeau (39). After concentration to 5 mg/ml by Amicon filtration, this fraction gave a single peak on a Superose 6 chromatography.

In conclusion, 2–3 mg of highly homogeneously purified protein, as assessed by both SDS-PAGE and Superose 6 chromatography, was obtained from 1.5 liters of yeast culture. It should also be stressed that up to 50 mg of a largely pure and very active 84-kDa protein could be obtained rapidly by a simple heat shock treatment of the solubilized particulate fraction (Table I).

*The Structure of MJ1226p Is Compatible with a P-type ATPase*—The Superose 6 chromatographed and purified fraction was analyzed by electron microscopy, appearing monodisperse, with no aggregates. Fig. 3*A* showed a representative gallery of MJ1226p negatively stained particles. Average image of the major class identified in the whole population revealed a 2-fold symmetrical structure with two distinct domains (Fig. 3*B*). A first domain (Fig. 3*B*, *arrow*) was roughly elliptical with a constant 4.0 nm size in minor axis, variable size in major axis, and presenting high variance values at both extremities. This domain could be compatible with the transmembrane hydrophobic regions of the protein embedded in a detergent micelle. A second domain (Fig. 3*B*, *arrowhead*) corresponded to a 7.5 nm height hydrophilic domain, protruding out of the detergent micelle and composed of two identical motifs. Each motif was made of a square stalk, having 1.5 nm inside, finishing by two contiguous globular densities of 2.5 and 3.5 nm in diameter.

The three-dimensional reconstruction at 2.4 nm resolution, performed on frozen-hydrated specimens, is shown in Fig. 3*C*. Lateral view (denoted by *1*) of the surface representation has been placed in an orientation similar to that of the average image shown in Fig. 3*B*. This view clearly demonstrated a dimeric organization of MJ1226p. Fig. 3*C*, *top view* (denoted by

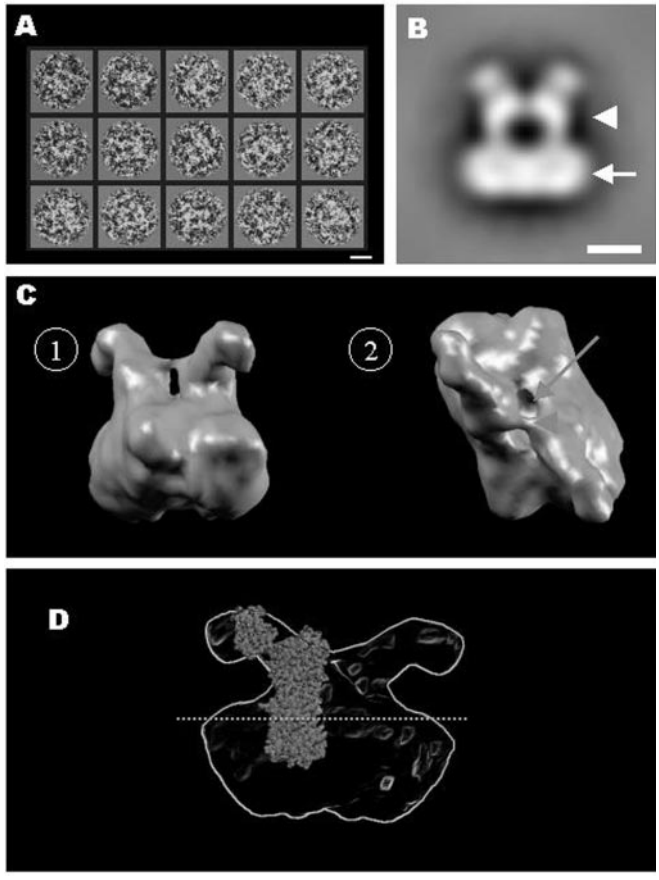


FIG. 3. **Electron microscopy and three-dimensional reconstruction of MJ1226p.** *A*, representative gallery of MJ1226p negatively stained particles. *Scale bar* 5 nm. *B*, average image of the major class identified in the whole population revealing a 2-fold symmetrical structure possessing two domains. A first domain (*arrow*) corresponds to the detergent-embedded transmembrane helices of the protein. A second domain (*arrowhead*), 7.5 nm in height, is composed of two identical motifs. *Scale bar* 5 nm. *C*, lateral view (denoted by *1*) of the surface representation, placed in an orientation similar to that of the average image in *B* demonstrating a dimeric organization of MJ1226p. *Top view* (denoted by *2*), indicated the presence of a cylindrical central cavity (*arrow*) of ~2.5 nm in diameter, between each monomer. *D*, docking of the $Ca^{2+}$-ATPase atomic structure into a MJ1226p monomer.

*2*), indicated the presence of a cylindrical central cavity of ~2.5 nm in diameter between each monomer (*arrow*).

Docking the atomic model of the sarcoplasmic reticulum $Ca^{2+}$-ATPase (21) within each monomer in the three-dimensional reconstruction shows that the large cytoplasmic domain of the $Ca^{2+}$-ATPase, consisting of 3 domains called A (transduction domain), N (ATP binding domain), and P (phosphorylation domain), connected to the transmembrane region by long loops, looked very similar to the 7.5 nm height hydrophilic domain of MJ1226p, protruding out of the detergent micelle in which the 10 transmembrane $\alpha$-helices are embedded (Fig. 3*D*). Similar results were obtained when a MJ1226p model was computed from sequence alignment with the $Ca^{2+}$-ATPase and modeler software applied (40). Thus, due to the low resolution obtained in this work, the 20% difference in mass between $Ca^{2+}$-ATPase and MJ1226p did not change the total surface (data not shown). On the other hand, comparison of the atomic structure of the $Ca^{2+}$-ATPase to the 8-Å three-dimensional map of the plasma $H^+$-ATPase indicated that both P-type ATPases had similar overall dimensions, that their transmembrane parts looked very similar, but that they could differ substantially in their cytoplasmic domains due to conformational states as part of the E1-E2 transition (41). In this context, the higher mass density observed in the hydrophilic 3.5 nm globular domains of the three-dimensional reconstruction of MJ1226p, when compared with the $Ca^{2+}$-ATPase model, could not be related to a conformational state but rather to an oversampling of the MJ1226p frontal views.

*Functional Characterization of MJ1226p*—All functional characterization was performed on pure protein preparations obtained by Superose 6 chromatography after heat shock and Ni-NTA chromatography. However, preparations from a single heat treatment, although of lower specific activity (50 $\mu$mol·min$^{-1}$·mg$^{-1}$), exhibited all the biochemical properties described for the purified protein preparation.

*Dependence of MJ1226p-ATPase Activity on Detergent*—As for most membrane proteins solubilized in detergent, MJ1226p requires the inclusion of optimized amounts of detergents or lipids in the assay medium to be fully functional. In the absence of DDM added to the assay medium, no ATPase activity could be measured. This lost of activity was prevented by addition of different phospholipids in the assay medium. The purified MJ1226p ATPase showed activities of 70–100 $\mu$mol·min$^{-1}$·mg$^{-1}$ when assayed in the presence of 0.05% asolectin, phosphatidylethanolamine, or phosphatidylcholine. The effects of different detergents upon restoring the ATPase activity were also tested by diluting the purified protein in buffers containing different detergents at concentrations above their critical micellar concentration, in replacement of the phospholipids. Among them, DDM was the most efficient and yielded maximal ATPase activities of about 150–180 $\mu$mol·min$^{-1}$·mg$^{-1}$. Other detergents, including *n*-octyl-$\beta$-D-glucopyranoside, Triton X-100, lauryldimethylamine oxide, Nonidet, CHAPS, or deoxycholate, were much less active, leading to only 1–8% of the ATPase activity measured in DDM. Only Zwittergent 2-14 provided intermediate activity (49% of the ATPase activity measured in DDM).

*Dependence of MJ1226p-ATPase Activity on Temperature, pH, and Monovalent Ions*—Fig. 4 showed the dependence of MJ1226p ATPase activity on temperature. Considering that under physiological conditions this enzyme operates at very high temperature, it was not surprising that MJ1226p was inactive below 40 °C. For temperatures above 40 °C, ATPase activity increased drastically to reach a maximum specific activity at about 95 °C. At this high temperature, ATPases activities above 150 $\mu$mol·min$^{-1}$·mg$^{-1}$ could be measured (Fig. 4*B*).

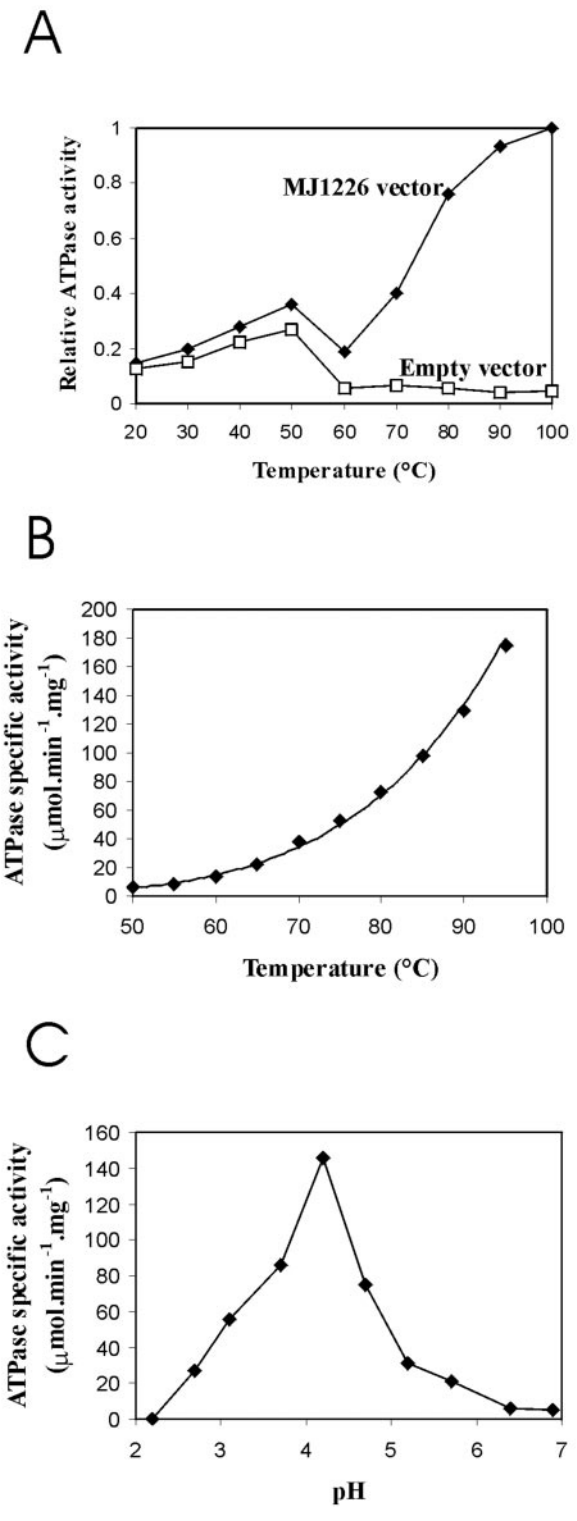


FIG. 4. **Dependence of MJ1226p ATPase activity on temperature and pH.** Standard ATPase assays were performed using a buffer containing 200 mM potassium acetate, 6 mM Mg ATP, and 50 mM Mes-KOH at the desired pH. *A*, total ATPase activities of crude membrane fractions (75 $\mu$g of protein) of uninduced and induced *S. cerevisiae* determined at different temperatures. *B*, ATPase activities of the purified MJ1226p determined at different temperatures. *C*, ATPase activities of the purified MJ1226p determined at 95 °C and different pH values (measured at 95 °C).

In the presence of DDM and monovalent salts (see below), the energy of activation (*Ea*) for MJ1226p hydrolytic ATPase activity, calculated between 40 and 80 °C, was about 75 kJ/mol. This value was similar to that obtained with other thermophilic

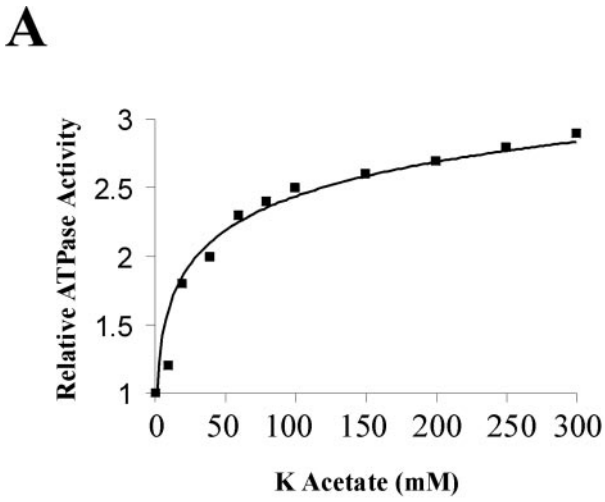


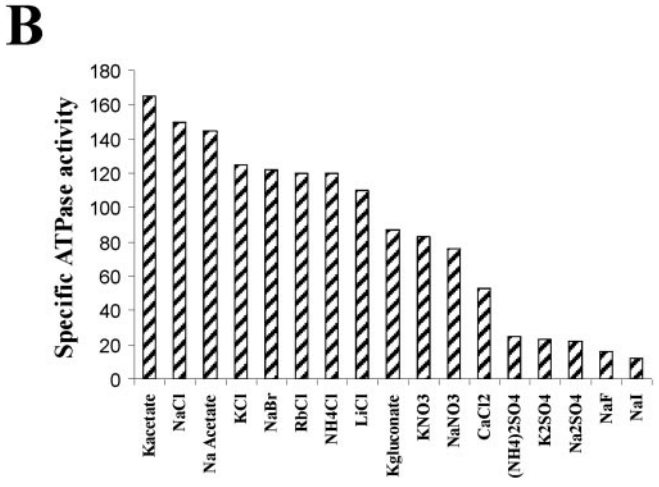


FIG. 5. **Dependence of MJ1226p ATPase activity on monovalent salts.** *A*, MJ1226p ATPase activities were measured at 95 °C in the presence of 0.1% DDM and different concentrations of potassium acetate. The reaction mixture was as under "Materials and Methods." The 50 mM Mes-KOH, pH 5.0 buffer, contained about 25 mM KOH and the 0.1% DDM contained about 2 mM $Na^+$. The relative stimulation of 1.0 corresponds to 62 $\mu$mol·min$^{-1}$·mg$^{-1}$ observed in 50 mM Mes-KOH and no added salt. Similar values were obtained with 50 mM Mes-Tris. *B*, MJ1226p ATPase Activities were measured with 50 mM Mes-KOH, pH 5.0, 0.1% DDM at 95 °C, in the presence of 200 mM of different salts. The basic ATPase activity, in presence of 50 mM Mes-KOH, 0.1% DDM but without added salt, is 62 $\mu$mol·min$^{-1}$·mg$^{-1}$.

enzymes (11, 42) and much higher than the 20–30 kJ/mol energy of activation generally reported for mesophilic soluble enzymes (43).

MJ1226p showed a typical bell-shaped dependence activity on pH with a maximum activity at pH 4.2 (Fig. 4*C*). Noteworthy, this optimal pH appeared significantly more acidic compared with the *S. pombe* $H^+$-ATPase (SpPMA1) and to the *A. fulgidus* $Ag^+/Cu^+$-ATPase whose optimal activities have been reported at pH 6.0–6.5 (11, 44).

High salt concentration stimulated the ATPase, reaching a plateau at 200–300 mM salt (Fig. 5*A*). This effect appears rather independent of the cation because NaCl, KCl, RbCl, $NH_4Cl$, or LiCl yielded similar ATPase stimulations. On the other hand, the anion specificity appeared more drastic because monovalent anions, such as $F^-$ and $I^-$, as well as the divalent anion $SO_4^{2-}$ inhibited ATPase activities as compared with $COO^-$, $Cl^-$, $Br^-$, $NO_3^-$, and gluconate$^-$ (Fig. 5*B*).

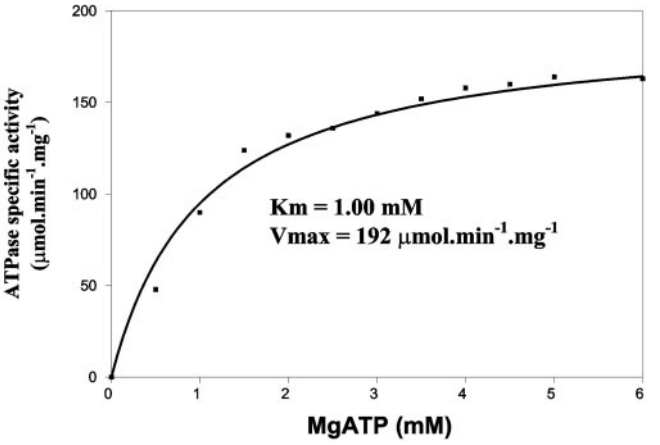


FIG. 6. **ATP dependence of MJ1226p ATPase activity.** ATPase activity was determined as described under "Materials and Methods" and MgATP concentration varied as indicated.

*Kinetics and Inhibitors of MJ1226p ATPase*—The major nucleotidic substrate of MJ1226p is MgATP. Little activity was observed for other nucleotides such as ITP, GTP, CTP, UTP, or ADP (data not shown). Divalent cations, other than magnesium, could complex ATP. When the total ATP concentration was fixed at 6 mM and the total divalent cation concentrations at 10 mM of chloride salts, the following order of activity was observed: cobalt (100%), magnesium (98%), manganese (80%), nickel (60%), zinc (50%), cadmium (40%), and calcium (15%) (not shown).

The MgATP hydrolysis followed a simple Michaelis-Menten relation leading to a $K_m$ of 1.0 mM MgATP and a $V_{max}$ of 192 $\mu$mol·min$^{-1}$·mg$^{-1}$ (Fig. 6).

Different ATPases inhibitors were tested. Table II shows that 1.5 mM NaF, to which P-type ATPases are usually resistant, inhibited 50% of the MJ1226p ATPase activity. The MJ1226p ATPase was moderately sensitive to the classical P-type inhibitor vanadate with an $I_{50}$ of 0.9 mM at pH 4.2. The low sensitivity to vanadate was largely due to the acid pH used for the assay, which is known to convert vanadate to non-inhibitory forms (45). At pH 5.2, the $I_{50}$ measured for vanadate was 250 $\mu$M. Fluorescein isothiocyanate, which is known to bind to the lysine residue of the conserved motif KGAP of P-type ATPases, inhibited up to 50% of the purified MJ1226p ATPase activity at the low concentration of 75 $\mu$M. The sulfhydryl reagent, *p*-chloromercuribenzoate ($I_{50}$ of 5 $\mu$M), was a powerful inhibitor of MJ1226p ATPase activity, whereas *N*-ethylmaleimide was much less active.

*Stability of MJ1226p ATPase*—MJ1226p ATPase was highly resistant to chaotropic agents. The presence of 200 mM guanidine hydrochloride was stimulatory, whereas 1 M guanidine hydrochloride inhibited only 50% of the MJ1226p ATPase activity. By comparison, the purified *S. pombe* PMA1 $H^+$-ATPase was much more sensitive because 50% of its ATPase activity was inhibited by 200 mM guanidine hydrochloride (Fig. 7). MJ1226p ATPase activity was also remarkably resistant to urea because only 50 and 60% inhibition were observed in the presence of 2.5 and 4.0 M urea, respectively. The *S. pombe* PMA1 ATPase was slightly more sensitive to urea because its ATPase activity was inhibited by 75% in the presence of 4 M urea. In contrast, the MJ1226p enzyme was inhibited by moderate $Me_2SO$ concentrations ($I_{50}$ of 15%).

The MJ1226p ATPase was extremely stable upon long storage at temperatures ranging from −4 °C to +65 °C. In particular, similar activities were found after storage of the purified protein for more than 1 week at +65 °C. On an other hand, the purified preparation could be frozen at −20 or −80 °C for

TABLE II
*Inhibitors of MJ1226p ATPase*

The abbreviations used are as follows: *p*CmB, *p*-chloromercuribenzoate; NEM, *N*-maleimide; FITC, fluorescein isothiocyanate

| Inhibitors | $I_{50}$ |
|---|---|
| *p*CMB | 5 μM |
| SDS | 0.05% |
| NaF | 1.5 mM |
| NEM | 50 mM |
| Vanadate | 0.9 mM |
| FITC | 75 μM |
| $Me_2SO$ | 15% |

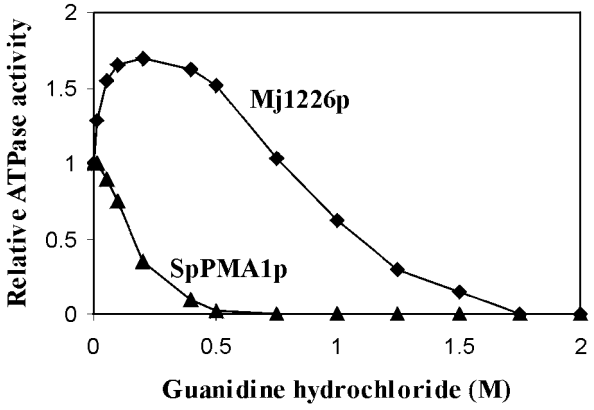


FIG. 7. **Stability of MJ1226p ATPase activity to guanidine hydrochloride.** ATPase activity was determined at 95 and 30 °C for purified MJ1226p and *S. pombe* PMA1p (SpPMA1p), respectively. Guanidine hydrochloride concentration was varied as indicated.

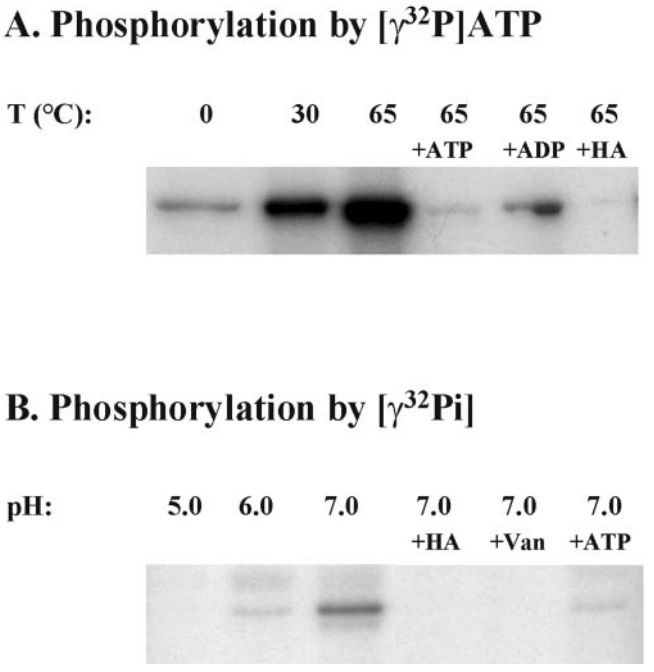


FIG. 8. **Phosphorylation by ATP or $P_i$ of purified MJ1226p.** Ten μg of purified MJ1226p was phosphorylated either by 2 mM [γ-$^{32}$P]ATP for 1 s (*A*) or by 5 mM [$^{32}P_i$] for 10 min (*B*) at the indicated temperature, pH, and inhibitor.

months and submitted to at least 4 freeze and thaw cycles without any loss of activity.

*MJ1226p Forms a Catalytic Phosphorylated Intermediate*—The purified MJ1226p ATPase was incubated with [γ-$^{32}$P]ATP at different temperatures and analyzed by gel electrophoresis (Fig. 8*A*). A phosphorylated band around 84 kDa was observed, the intensity of which increased with temperature. For comparison, a *S. pombe* ATPase preparation also showed a phosphorylated band at 100 kDa, whose intensity increased from 0 to 30 °C but was not detectable at 65 °C, probably because of the heat denaturation of this mesophilic enzyme (data not shown). The radioactivity signals were not due to the unspecific binding of [γ-$^{32}$P]ATP on the protein because [α-$^{32}$P]ATP did not phosphorylate MJ1226p nor SpPMA1 (not shown). Phosphorylation of MJ1226p was inhibited by preincubation of the protein with 1 mM ADP (Fig. 8*A*). Treatment of the phosphorylated MJ1226p with either 10 mM cold ATP or with 10 mM hydroxylamine also reduced the signal to near-background level (Fig. 8*A*).

MJ1226p could also be phosphorylated by $P_i$ (Fig. 8*B*). The phosphorylation level increased with the pH between pH 5.0 and 7.0 (Fig. 8*B*). Phosphorylation by $P_i$ was inhibited by preincubation of MJ1226p with vanadate or by treatment of the phosphorylated protein with hydroxylamine (Fig. 8*B*). Addition of 1 mM MgATP at the end of the assay released fixed $P_i$ leading to a decrease of the phosphorylation level (Fig. 8*B*). These properties are those expected for a P-type ATPase.

## DISCUSSION

In the last decade, genomic studies of different archaebacteria have brought attention to their membrane proteins. Many of them were found to be new members of phylogenetic subfamilies containing eucaryotic proteins. The high stability of archaeal membrane proteins to extreme temperature, pressure, or pH could overcome the experimental bottlenecks often encountered for solubilization and purification of their eucaryotic homologs. Indeed, these steps necessitate long time exposure to detergents, which is often deleterious for many membrane proteins from eucaryotic cells. In addition, the possibility to overexpress large amounts of stable archaeal membrane proteins from wild type but also from mutant genes open novel perspectives for structural studies through crystallization trials.

We report here on the expression in *S. cerevisiae* and on the large scale purification of a P-type ATPase from the hyperthermophilic Archaea *M. jannaschii.* By using a cloning system that was shown to be suitable for heterologous expression of plant and fungi plasma membrane $H^+$-ATPases, we have been able to express the archaeal *MJ1226* gene in the yeast *S. cerevisiae*. The drastic purification of MJ1226p by a treatment of the total solubilized extract for 5 min at 95 °C was particularly convenient, leading to the production of up to 50 mg of a pure and very active protein per liter of yeast culture. A subsequent Ni-NTA chromatography was also efficient and increased considerably the ATPase activity of the heat-treated solubilized MJ1226p. The combination of the heat treatment and of the Ni-NTA chromatography yielded only one 84-kDa polypeptide component as detected on silver-stained SDS-PAGE gels. Finally, a subsequent size-exclusion gel chromatography allowed the production of a highly monodisperse protein preparation. The complete isolation procedure routinely yielded 2 mg of more than 95% pure protein per liter of yeast culture, with specific ATPase activities as high as 180 $\mu mol \cdot min^{-1} \cdot mg^{-1}$ at 95 °C. The specific activity of the *M. jannaschii* enzyme expressed in yeast was 700 times higher than the activity of the $Ag^+/Cu^+$-ATPase from *A. fulgidus* expressed in bacteria (11). Another striking feature of the purified MJ1226p was its high stability upon freeze/thawing or long storage at 4–65 °C and its high resistance to chaotropic agents such as urea and guanidine hydrochloride. This stability and high yield of homogenous MJ1226p purified from crude membranes were particularly convenient for biochemical, kinetic, biophysical, and structural characterizations. Its expression in

*S. cerevisiae* and lack of toxicity also enables future studies of MJ1226p mutants.

Blast analysis of the MJ1226p sequence revealed high similarity between membrane proteins from the P-type ATPase superfamily. These predictions were confirmed by functional and structural analyses performed on the purified MJ1226p. A primary characteristic of P-type ATPases is their ability to form an aspartyl-phosphate catalytic intermediate (as shown for the yeast (26) and plant (46) $H^+$-ATPases). Here we demonstrated that the archaeal MJ1226p ATPase was able to form a hydroxylamine-sensitive phosphoenzyme catalytic intermediate from radioactive ATP. This phosphorylation was inhibited by addition of ADP and reduced to near-background levels by addition of cold ATP. The phosphorylation of MJ1226p by inorganic phosphate, which is a partial reverse step of the catalytic cycle, was much more active than in fungal proton ATPases where the catalytic cycle is largely irreversible (47). We showed both phosphorylation activities operating at 30 °C, and these activities were much less dependent on high temperature than the MJ1226p ATPase activity, which does not function at all at 30 °C. This suggests that the correct enzyme conformation reached at high temperature mostly concerns the transition of the unphosphorylated *E*1 state from the dephosphorylated *E*2 state. Besides its capacity to form an aspartyl-phosphate intermediate, MJ1226p ATPase activity is also inhibited by vanadate, which is a characteristic feature of P-type ATPases. A third argument for MJ1226p belonging to the P-type ATPase family is the three-dimensional reconstruction of the detergent-solubilized MJ1226p deduced from our single particle analysis by electron microscopy. Although at a 2.5 nm resolution, the structure of the purified MJ1226p was compatible with the atomic structure of the $Ca^{2+}$-ATPase. Other functional properties of MJ1226p were compatible with those found in other plasma membrane P-type ATPases. The substrate specificity for MgATP, the $K_m$ and $V_{max}$ values, the inhibition by fluorescein isothiocyanate, and sulfhydryl reagents compounds were in the same range as those reported for the other P-type ATPases.

From the highest sequence similarity with plant and yeast plasma membrane $H^+$-ATPases, MJ1226p had been phylogenetically classified in the family of plasma membrane $H^+$-ATPases (36). However, the phylogenetic link showing 40% sequence identity with proton-transporting ATPase is not an overwhelming argument that MJ1226p ATPase transports protons. Among other credible possibilities, MJ1226p could be a novel $Na^+$ (or $K^+$) transporter. The strong stimulation of MJ1226p ATPase activity by sodium and potassium monovalent salts would be coherent with a sodium pumping function. A final answer to this question will be given by successful *in vitro* experiments, which are currently in progress in our laboratory, to reconstitute proteoliposomes able to maintain a pH gradient above 65 °C. Whatever the final interpretation, the presence of a very active putative $H^+$ (and/or $Na^+$)-ATPase in *M. jannaschii* (and possibly of *Thermoplasma acidophilum*) strongly indicates a role for these pumps in the setting of the proton- or sodium-motive force that should be key elements for the survival of these Archaea species growing at high salt or low pH conditions. In this context, evidence for $H^+$- or $Na^+$-mediated chemiosmotic transduction pathways has been reported in methanogens (48).

We have shown that MJ1226p expressed in *S. cerevisiae* retained its thermophilic properties with an optimal activity above 95 °C, compatible with the growth conditions required for *M. jannaschii* in the fumes of undersea volcanoes. This thermophilic ATPase seems to share similar catalytic mechanisms with their mesophilic P-type ATPase homologs (49). Sequence alignment, amino acid content comparisons, and crystal structure comparisons indicate that thermostable proteins are often similar to their mesophilic homologues (49). We could not observe strong divergence between the amino acid sequence of MJ1226p and the other plant and fungi $H^+$-ATPases, indicating that thermostability was probably caused by the accumulation of numerous subtle sequence differences modifying the intrinsic stabilizing forces of the proteins (*e.g.* salt bridges, hydrogen bonds, hydrophobic interactions) (50). In this context, the resistance to chaotropic agents could also reflect a compact hydrophobic structure of the enzyme that would be relaxed only by high temperature to reach its optimal activity.

In conclusion, high amounts of active, homogeneous, and stable protein has been made available for further biophysical, structural, and mutagenic studies of the MJ1226p P-type ATPase expressed in yeast. Whether other thermophilic Archaea P-type ATPases can be produced in yeast with equal success is under investigation.

*Acknowledgments*—We thank Brian Monk (Ottago, New Zealand) and Daniel Levi (Institut Curie, Paris, France) for suggestions and discussions.

REFERENCES

1. Lancaster, J. R., Jr. (1989) *J. Bioenerg. Biomembr.* **21,** 717–740
2. Schafer, G., Engelhard, M., and Muller, V. (1999) *Microbiol. Mol. Biol. Rev.* **63,** 570–620
3. Bult, C. J., White, O., Olsen, G. J., Zhou, L., Fleischmann, R. D., Sutton, G. G., Blake, J. A., FitzGerald, L. M., Clayton, R. A., Gocayne, J. D., Kerlavage, A. R., Dougherty, B. A., Tomb, J. F., Adams, M. D., Reich, C. I., Overbeek, R., Kirkness, E. F., Weinstock, K. G., Merrick, J. M., Glodek, A., Scott, J. L., Geoghagen, N. S., and Venter, J. C. (1996) *Science* **273,** 1058–1073
4. Ruepp, A., Graml, W., Santos-Martinez, M. L., Koretke, K. K., Volker, C., Mewes, H. W., Frishman, D., Stocker, S., Lupas, A. N., and Baumeister, W. (2000) *Nature* **407,** 508–513
5. Dufour, J. P., and Goffeau, A. (1978) *J. Biol. Chem.* **253,** 7026–7032
6. Malpartida, F., and Serrano, R. (1980) *FEBS Lett.* **111,** 69–72
7. Addison, R., and Scarborough, G. A. (1981) *J. Biol. Chem.* **256,** 13165–13171
8. Bowman, E. J., Bowman, B. J., and Slayman, C. W. (1981) *J. Biol. Chem.* **256,** 12336–12342
9. Harper, J. F., Surowy, T. K., and Sussman, M. R. (1989) *Proc. Natl. Acad. Sci. U. S. A.* **86,** 1234–1238
10. Boutry, M., Michelet, B., and Goffeau, A. (1989) *Biochem. Biophys. Res. Commun.* **162,** 567–574
11. Mandal, A. K., Cheung, W. D., and Arguello, J. M. (2002) *J. Biol. Chem.* **277,** 7201–7208
12. Horowitz, B., Eakle, K. A., Scheiner-Bobis, G., Randolph, G. R., Chen, C. Y., Hitzeman, R. A., and Farley, R. A. (1990) *J. Biol. Chem.* **265,** 4189–4192
13. Pedersen, A., and Jorgensen, P. L. (1992) *Ann. N. Y. Acad. Sci.* **671,** 542–544
14. Centeno, F., Deschamps, S., Lompre, A. M., Anger, M., Moutin, M. J., Dupont, Y., Palmgren, M. G., Villalba, J. M., Moller, J. V., Falson, P., and Lemaire, M. (1994) *FEBS Lett.* **354,** 117–122
15. de Kerchove d'Exaerde, A., Supply, P., Dufour, J. P., Bogaerts, P., Thines, D., Goffeau, A., and Boutry, M. (1995) *J. Biol. Chem.* **270,** 23828–23837
16. de Kerchove d'Exaerde, A., Morsomme, P., Sempoux-Thines, D., Supply, P., Goffeau, A., and Ghislain, M. (1997) *Mol. Microbiol.* **25,** 261–273
17. Talla, E., de Mendonca, R. L., Degand, I., Goffeau, A., and Ghislain, M. (1998) *J. Biol. Chem.* **273,** 27831–27840
18. Degand, I., Catty, P., Talla, E., Thines-Sempoux, D., de Kerchove d'Exaerde, A., Goffeau, A., and Ghislain, M. (1999) *Mol. Microbiol.* **31,** 545–556
19. Morsomme, P., and Boutry, M. (2000) *Biochim. Biophys. Acta* **1465,** 1–16
20. Auer, M., Scarborough, G. A., and Kuhlbrandt, W. (1998) *Nature* **392,** 840–843
21. Toyoshima, C., Nakasako, M., Nomura, H., and Ogawa, H. (2000) *Nature* **405,** 647–655
22. Gietz, R. D., and Sugino, A. (1988) *Gene* (*Amst.*) **74,** 527–534
23. Ito, H., Fukuda, Y., Murata, K., and Kimura, A. (1983) *J. Bacteriol.* **153,** 163–168
24. Goffeau, A., and Dufour, J. P. (1988) *Methods Enzymol.* **157,** 528–533
25. Lowry, O. H., Rosebrough, N. J., Farr, A. L., and Randall, R. J. (1951) *J. Biol. Chem.* **193,** 265–275
26. Amory, A., Foury, F., and Goffeau, A. (1980) *J. Biol. Chem.* **255,** 9353–9357
27. Marabini, R., Masegosa, I. M., San Martin, C., Marco, S., Fernandez, J. J., de la Fraga, L. G., Vaquerizo, C., and Carazo, J. M. (1996) *J. Struct. Biol.* **116,** 237–240
28. Marco, S., Chagoyen, M., Fraga, L. G., Carazo, J. M., and Carrascosa, J. L. (1996) *Ultramicroscopy* **66,** 5–10
29. Marabini, R., and Carazo, J. M. (1994) *Biophys. J.* **66,** 1804–1814
30. van Hell, M., and Frank, J. (1981) *Ultramicroscopy* **6,** 187–194
31. van Heel, M. (1984) *Ultramicroscopy* **13,** 165–183
32. Frank, J., Radermacher, M., Penczek, P., Zhu, J., Li, Y., Ladjadj, M., and Leith, A. (1996) *J. Struct. Biol.* **116,** 190–199
33. Dubochet, J., Adrian, M., Chang, J. J., Homo, J. C., Lepault, J., McDowall, A. W., and Schultz, P. (1988) *Q. Rev. Biophys.* **21,** 129–228
34. Saxton, W. O., and Baumeister, W. (1982) *J. Microsc.* **127,** 127–138
35. Mullick, R., Venkataraman, S., Warusavithana, S., Nguyen, H. T., and

Raghavan, R. (1998) *Annual Meeting of the Society for Computer Applications in Radiology*
36. Axelsen, K. B., and Palmgren, M. G. (1998) *J. Mol. Evol.* **46,** 84–101
37. Bukrinsky, J. T., Buch-Pedersen, M. J., Larsen, S., and Palmgren, M. G. (2001) *FEBS Lett.* **494,** 6–10
38. Morsomme, P., de Kerchove d'Exaerde, A., De Meester, S., Thines, D., Goffeau, A., and Boutry, M. (1996) *EMBO J.* **15,** 5513–5526
39. Dufour, J. P., and Goffeau, A. (1980) *J. Biol. Chem.* **255,** 10591–10598
40. Fiser, A., Do, R. K., and Sali, A. (2000) *Protein Sci.* **9,** 1753–1773
41. Stokes, D. L., Auer, M., Zhang, P., and Kuhlbrandt, W. (1999) *Curr. Biol.* **9,** 672–679
42. Hinrichs, M., Schafer, G., and Anemuller, S. (1999) *Biol. Chem.* **380,** 1063–1069
43. Segel, I. H. (1993) *Enzyme Kinetics*, John Wiley & Sons Ltd., Chichester, UK
44. Dufour, J. P., and Goffeau, A. (1980) *Eur. J. Biochem.* **105,** 145–154
45. Borst-Pauwels, G. W., and Peters, P. H. (1981) *Biochim. Biophys. Acta* **642,** 173–181
46. Vara, F., and Serrano, R. (1983) *J. Biol. Chem.* **258,** 5334–5336
47. de Meis, L., Blanpain, J. P., and Goffeau, A. (1987) *FEBS Lett.* **212,** 323–327
48. Deppenmeier, U., Lienard, T., and Gottschalk, G. (1999) *FEBS Lett.* **457,** 291–297
49. Vieille, C., Burdette, D. S., and Zeikus, J. G. (1996) *Biotechnol. Annu. Rev.* **2,** 1–83
50. Jaenicke, R. (1996) *FASEB J.* **10,** 84–92
51. Palmgren, M. G. (2001) *Annu. Rev. Plant. Physiol. Plant. Mol. Biol.* **52,** 817–845